FEATURE ARTICLE
Search for Color 'Center(s)' in Macaque Visual Cortex

Roger B.H. Tootell[1], Koen Nelissen[2], Wim Vanduffel[1,2] and Guy A. Orban[2]

[1]Nuclear Magnetic Resonance Center, Massachusetts General Hospital and Department of Radiology, Harvard Medical School, Boston, MA 02115, USA and [2]Laboratorium voor Neuro- en Psychofysiologie, KU Leuven Medical School, Leuven B 3000, Belgium
The first three authors contributed equally to this study.

It is often stated that color is selectively processed in cortical area V4, in both macaques and humans. However most recent data suggests that color is instead processed in region(s) antero-ventral to V4. Here we tested these two hypotheses in macaque visual cortex, where 'V4' was originally defined, and first described as color selective. Activity produced by equiluminant color-varying (versus luminance-varying) gratings was measured using double-label deoxyglucose in awake fixating macaques, in multiple areas of flattened visual cortex. Much of cortex was activated near-equally by both color- and luminance-varying stimuli. In remaining cortical regions, discrete color-biased columns were found in many cortical visual areas, whereas luminance-biased activity was found in only a few specific regions (V1 layer 4B and area MT). Consistent with a recent hypothesis, V4 was not uniquely specialized for color processing, but areas located antero-ventral to V4 (in/near TEO and anterior TE) showed more color-biased activity.

Keywords: color, double label deoxyglucose, monkey, V4

Introduction

Some aspects of primate vision are 'modular': processed in (partially) segregated channels within the brain. For instance in cerebral cortex, visual motion cues are processed selectively (though not exclusively) in specific layers (e.g. layer 4B of V1), areas (e.g. MT, MST) and columns (Albright *et al.*, 1984; Malonek *et al.*, 1994; Geesaman *et al.*, 1997).

However the hypothesis of modularity is more controversial in other stimulus dimensions, such as color. For instance, in primary visual cortex (V1) it has been reported that color is processed selectively in specialized anatomical compartments (the 'blobs') (Livingstone and Hubel, 1984; Tootell *et al.*, 1988; Landisman and Ts'o, 2002) but this claim has been disputed (Lennie *et al.*, 1990; Leventhal *et al.*, 1995) and qualified (Yoshioka and Dow, 1996). A similar controversy persists in area V2, where color may (Hubel and Livingstone, 1987; Roe and Ts'o, 1999; Tootell and Hamilton, 1989; Moutoussis and Zeki, 2002; DeYoe *et al.*, 1994; Xiao *et al.*, 2003) or may not (Levitt *et al.*, 1994; Kiper *et al.*, 1997) be selectively processed in the thin dark cytochrome oxidase (CO) stripes.

Further anterior in extrastriate cortex, the main color-related controversy has centered on area V4, for more than three decades. During this time, several sub-issues emerged (for a review, see Tootell *et al.*, 2003). For instance, are single units in macaque V4 color-selective (Zeki, 1973, 1977) or not (Kruger and Gouras, 1980; Van Essen *et al.*, 1981; Fischer *et al.*, 1981; Schein *et al.*, 1982)? Are 'V4d' and 'V4v' really retinotopic subdivisions of a common area 'V4' (Van Essen and Zeki, 1978; Gattass *et al.*, 1988), or not (Tootell and Hadjikhanim, 2001; Fize *et al.*, 2003)? Is the main color-selective region in

human visual cortex homologous with macaque area V4 (Lueck *et al.*, 1989; McKeefry and Zeki, 1997; Bartels and Zeki, 2000), or a different area further anterior (Hadjikhani *et al.*, 1998; Beauchamp *et al.*, 1999; Van Essen *et al.*, 2001)? In macaque, is there one main color 'center' as originally proposed (Zeki, 1973, 1977), or more as suggested in human fMRI studies (Beauchamp *et al.*, 1999; Bartels and Zeki, 2000)?

In the macaque (where the relevant cortical areas were originally defined), the original proposal was that color is processed selectively in V4 (Zeki, 1973). A more recent hypothesis predicts that color is *not* processed selectively in V4, but it *is* processed in discrete regions(s) anteriorly, in/near TEO (Hadjikhani *et al.*, 1998; Tootell and Hadjikhanim, 2001; Van Essen *et al.*, 2001) and perhaps in related areas further anterior (Komatsu *et al.*, 1992; Buckley *et al.*, 1997). Here we used neuroimaging to test these two proposals about color processing in macaque. This approach allowed us to conduct a common color-luminance test simultaneously in many areas of visual cortex.

Functional activity was labeled in matched conditions, during presentation of an experimental (color-varying) and a control (luminance-varying) stimulus, using a recent version of the double-label deoxyglucose (2L-DG) technique (Geesaman *et al.*, 1997; Vanduffel *et al.*, 2000, 2002a). This technique has excellent spatial resolution (to resolve cortical columns, layers, and small visual areas), high functional sensitivity, and the two resultant activity maps are essentially independent of each other (see Methods). Unlike alternative functional labeling techniques, this deoxyglucose approach is not susceptible to vascular artifacts, and it yields data throughout the brain. Moreover, the 2L-DG technique can be used in awake behaving (rather than anesthetized) macaques.

Studies of color sensitivity often disambiguate *color* variations from the *luminance* variations that normally accompany them, by equating the luminance across all stimuli. Recently it has been recognized that macaque and human sensitivity curves differ significantly (Dobkins *et al.*, 2000), so one cannot extrapolate human equiluminance values to macaques. Here we empirically measured the actual 'equiluminance' values in each monkey's cortex using visual evoked potentials (VEPs). This ensured that our color-varying test stimuli were equal in luminance, for both the species and the individuals tested.

Materials and Methods

Surgery and Training

The procedures were similar to those described previously (Geesaman *et al.*, 1997; Vanduffel *et al.*, 2000, 2002a). Three male rhesus monkeys (*Macaca mulatta*) were tested. First, each was trained to restraint in a primate chair. The head of each monkey was fixed in place using a previously implanted stainless steel device. Eye

positions were measured using the scleral eye-coil technique. All surgical procedures conformed to the American and European Guidelines for the care and use of laboratory animals (for details, see Vanduffel *et al.*, 2002a). Muscle relaxants were not used.

Access to water was restricted during the period of testing, and behavioral control was achieved using operant conditioning. The monkeys were rewarded with drops of apple juice for maintaining fixation within a square-shaped central fixation window (1–2° on a side for training, 3° during the DG experiment). Multiple rewards were given at gradually decreased intervals within a given fixation period (maximally 64 s duration), to encourage progressively longer fixation by the monkey. The health status of the monkeys was closely monitored throughout the period of water restriction.

Visual Stimuli

Stimuli were presented only when the monkey was steadily fixating the center of the screen. Each animal was presented with a color-varying grating (experimental stimulus) and an achromatic luminance-varying grating (control stimulus). The color-varying gratings varied along an axis between the purest 'red' and 'blue' values of the CRT screen. The achromatic luminance-varying grating varied around a white point calculated for the macaque. All gratings had a trapezoidal-shaped waveform, designed to incorporate the advantages of a square wave (which gives optimal contrast at each stimulated location) and a sine wave (which minimizes chromatic aberration at the 'edges' of each grating cycle) (see Fig. 1). All stimuli within a given experiment had a common mean luminance (5.9 cd/m² for white), which was luminance-equated for the macaque. Stimuli were presented on a Brilliance 21A Phillips monitor (70 Hz refresh rate), positioned 44 cm from the monkey's eyes. The stimuli subtended the full extent of the rectangular screen (50 × 36°).

In previous studies of color selectivity in macaque cortex, it has been common to test with CRT-based red–green color combinations. Here we instead tested with red–blue color combinations, for several reasons. First, the 'red' and 'blue' are actually closer to complementary colors than the 'red' and 'green', when comparing dominant wavelengths of the three CRT-based phosphors (~470, 543, 612 nm), in the human visual system. Second, the 'fundamental' human color axes (e.g. 'red–green') cannot be safely generalized to macaques, for the reasons described above (e.g. Dobkins *et al.*, 2000). Third, the blue phosphor is spectrally more pure, and probably more saturated, compared with the green phosphor. This is significant because an earlier DG study (Tootell *et al.*, 1988) showed that more saturated stimuli (e.g. blue compared with green) produce higher DG uptake in macaque V1.

In two cases (nos 1 and 3; see below) the color-varying grating was presented when [³H]DG was available in the bloodstream, and [¹⁴C]DG was injected into the bloodstream immediately after the luminance-varying presentation began. This order of presentation was reversed in the remaining case (no. 2), to ensure that the color-luminance differences were not confounded by order-of-presentation (or isotope-linked) differences. No such artifactual differences were found here, nor in previous studies with analogous controls (Vanduffel *et al.*, 2002a).

Within each of the three cases, all stimulus variables were equated, except for the experimental manipulation of color versus luminance. All gratings (both color- and luminance-varying) were of low spatial frequency (0.45 cycles/degree), because sensitivity to color is higher than to luminance in that spatial range, in human psychophysics (Van der Horst and Bouman, 1969; Granger and Heurtley, 1973; Watanabe *et al.*, 1976; Mullen, 1985) and macaque physiology (De Valois *et al.*, 1977; Hicks *et al.*, 1983; Thorell *et al.*, 1984; Kruger and Gouras, 1980).

Between cases, we varied several additional parameters, to encompass a range of typical grating configurations. This approach extended the generality of our basic color-luminance results. For instance in experiment 1, the grating was concentric, presented in continuous motion at 0.52 cycles/s. The direction of motion (centrifugal/centripetal) reversed every 32 s. Thus for a given location in visual space, this grating was effectively orientation-specific.
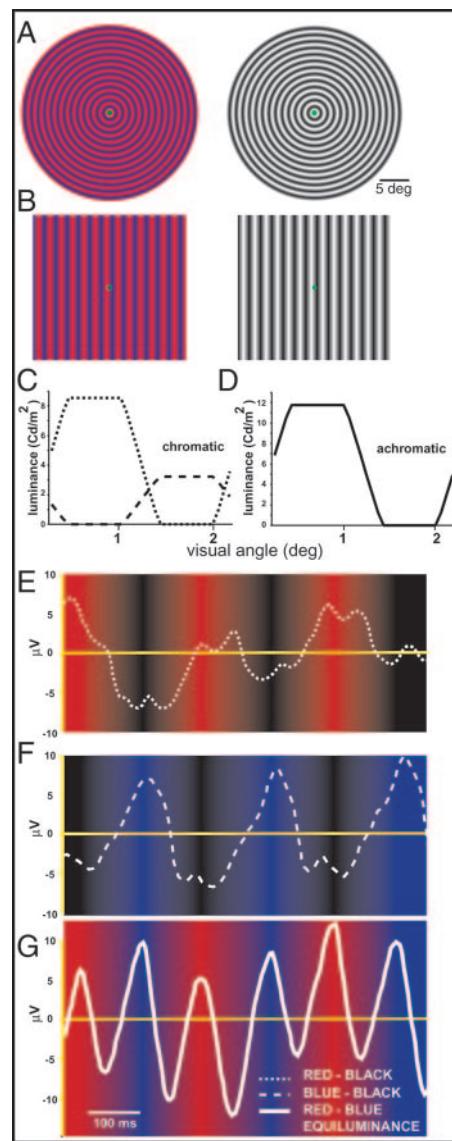

Figure 1. Stimuli and equiluminance tests. (*A*, *B*) The stimuli used in experiments 1 and 2–3, respectively. (*C*, *D*) The trapezoidal variation in color (dotted line = red; dashed line = blue) and luminance (respectively), across one spatial cycle of these gratings. (*E*–*G*) VEP responses, as the luminance of a red–blue stimulus was varied from the extremes of red–black (*E*) and blue–black (*F*), to 'equiluminant' red–blue (*G*). At this equiluminance ratio, the VEP response amplitudes to red and blue were essentially equal (*G*) and frequency-doubled, relative to the responses to either red–black (*E*) or blue–black (*F*).

In experiment 2, we used a conventional grating presented at a single (vertical) orientation, across the whole stimulus. Thus this grating was also orientation-specific. Technically, this grating did not move. Instead, to 'refresh' the activation, the phase of the grating was randomly changed at 4.4 Hz.

The stimulus for experiment 3 was equivalent to that in case 2, except that the grating orientation was systematically changed every 32 s, between four values spanning the orientation range (45, 90, 135 and 0/180°).

In all three cases, we were able to quantitatively compare the activation due to color, compared to that due to luminance. In case 3, that was the main variable we labeled, since orientation was systematically varied. In cases 1 and 2, the (constant-local-orientation) stimuli also produced corresponding orientation-selective columns in the individual-isotope maps, in areas V1, V2, V3 and VP (e.g. Vanduffel *et*

al., 2002a). However, in the *difference images* from these latter two cases, the orientation columns subtracted out, nearly completely (see Figs 3–5).

Functional Labeling and Histology
The double-label deoxyglucose (2L-DG) procedures are described elsewhere (Vanduffel *et al.*, 2000, 2002a; Geesaman *et al.*, 1997). Each isotope was injected intravenously (and remotely) while monkeys were awake and fixating to either experimental and control stimulus. A perfusion step removed unbound deoxyglucose. Before freezing, cortical tissue was physically flattened. Later the tissue block was cut parallel with the flattened cortical surface, to reveal images emphasizing the cortical topography. Selected sections were stained for cytochrome oxidase after autoradiography.

Visual area borders were estimated based on gyral/sulcal landmarks, DG-based functional and metabolic differences, histology (e.g. cytochrome oxidase), and retinotopy extrapolated from other individuals (e.g. Vanduffel *et al.*, 2002a,b; Fize *et al.*, 2003; R. Tootell, unpublished data). Residual uncertainties in area localization was estimated to be 1–2 mm in most cases; such uncertainty will be more significant in very thin areas such as V3/VP, but less important in larger areas such as V3A and V4d/v.

Imaging and Analysis
The autoradiographs corresponding to the ^{3}H- and ^{14}C-dominated images were digitized, registered, normalized and processed as described elsewhere (e.g. Vanduffel *et al.*, 2002a). The two isotope-linked activity maps were ~96% independent of each other, prior to any difference imaging. This near-independence was achieved by: (i) using a much higher ^{3}H:^{14}C ratio than in previous 2L-DG studies, by (ii) greatly truncating the period of second-isotope accumulation followed quickly by a perfusion step, and by (iii) using color film and filters for isotope separation in subsequent autoradiography and analysis.

Here additional statistical analysis was done, similar to that used in human neuroimaging studies (e.g. Worsley *et al.*, 1996). To restrict analysis to the tissue of interest, a digital mask was first calculated for the relevant portion of each section. Then a difference image was calculated for the aligned, normalized, ^{3}H- and ^{14}C-based images. The resultant image was smoothed (kernel size = 2 mm).

Detrending (removing the best fit linear trend from the data) was imposed in order to standardize the data, but this step did not change the ultimate result, except in a single tissue section. The standard error was calculated by subtracting the smoothed difference image from the difference image. This error map was smoothed with a kernel 10 times the width of the initial smoothing kernel. Next, the *t*-values were computed by dividing the smoothed difference image by the smoothed error. The minimum *t*-value was calculated for *P* < 0.05, corrected for multiple comparisons. For each pseudocolor scale, the maximum *t*-value was set to the highest value in the relevant difference image (usually, color minus luminance).

Equiluminance Measurements
In humans, VEP reversal potentials have been used as a physiological reflection of individual subjects' equiluminance values (Previc, 1986). Here we used this technique to define the equiluminance value of each monkey subject, in response to the exact colors used later in the test stimuli.

During the headset implantation, stainless steel skull screws were implanted directly over foveal striate cortex (3.5 cm along the skull from the posterior medial border, immediately dorsal to the nuccal ridge). Reference skull screws were implanted over frontal cortex. These skull screws were not fully covered with dental acrylic, so that later they could be accessed as VEP leads.

During a subsequent recording session, monkeys performed their fixation task while the amplitudes of these VEP signals were measured, in response to sinusoidal variations in the intensity of red and/or blue phosphor combinations, during stimulus counterphase at 4.4 Hz (see Fig. 1*E–G*). In the macaque, the maximum intensity of the red phosphor imposed the upper limit on the mean luminance used. To define equiluminance for the color-varying (red–blue) grating, the intensity of the blue phosphor was systematically varied until a 'reversal' point was found, at which the red and blue phosphors produced equal amplitude responses. The equiluminance value for white was set in the same way.

Results

Equiluminance Values
The VEP-based equiluminance values from different animals were quite similar to each other (red to blue ratio in cd/m^2 = 5.98, 6.24 and 5.33, in cases 1, 2 and 3, respectively). However, these macaque equiluminance ratios were also significantly different from analogous measurements in humans. This is consistent with a sensitivity shift to lower wavelengths in macaque as described previously (Dobkins *et al.*, 2000). However the luminance difference in our study was larger than in the previous report, because we used a color pair taken from the spectral extremes (red–blue), whereas Dobkins *et al.* (2000) tested a color pair spanning a smaller portion of the visible spectrum (red–green).

Behavior
The percentage of time that each monkey spent fixating was monitored continuously, in real time. The monkey's gaze remained within the central fixation window either 90, 85 and 95% of the time (average values, for experiments 1, 2 and 3, respectively). There were no significant differences in the average time the monkey spent fixating between the two isotope uptake periods.

Striate Cortex (Area V1)
Consistent with most previous evidence (see above), the *color*-varying gratings produced higher uptake in the upper layer blobs of layers 2 + 3 and adjacent layer 4A, compared to the control (luminance-varying) grating (see Fig. 2*A–C*). In the same animals, we found a strong *luminance* bias in magnocellular-dominated layer 4B (see Fig. 2*D–G*). For instance, in Figure 2*E* the (single-orientation) luminance-varying grating produced obvious orientation columns in layer 4B but analogous columns were almost negligible when the animal viewed the equiluminant color-varying grating (Fig. 2*D,F,G*). This 2L-DG-based 'color null' (minima) in layer 4B confirmed that our VEP-based equiluminance values selectively activated the chromatic pathway in macaque. Similar equiluminant color null responses have been reported in area MT (Dobkins *et al.*, 2000), to which layer 4B of V1 projects.

The elaborate laminar variation seen in V1 was largely absent in other areas. Throughout extrastriate cortex, the column contrast was highest in layer 4, tapering off gradually through both supra- and sub-granular layers.

Area V2
In V2, our 2L-DG results largely confirmed the 'classical' model of anatomically segregated color processing (see Fig. 3). In all three cases, color-driven DG activity was distinctly higher than luminance-driven activity within the thin dark CO stripes. More specifically, the DG color columns were localized to the small 'islands' of dark CO staining which comprise the so-called thin 'stripes'.

Within other regions of V2 (the pale 'interstripe' region and 'thick dark' CO stripes), luminance-driven activity was marginally higher than color activity. Consistent with prior reports
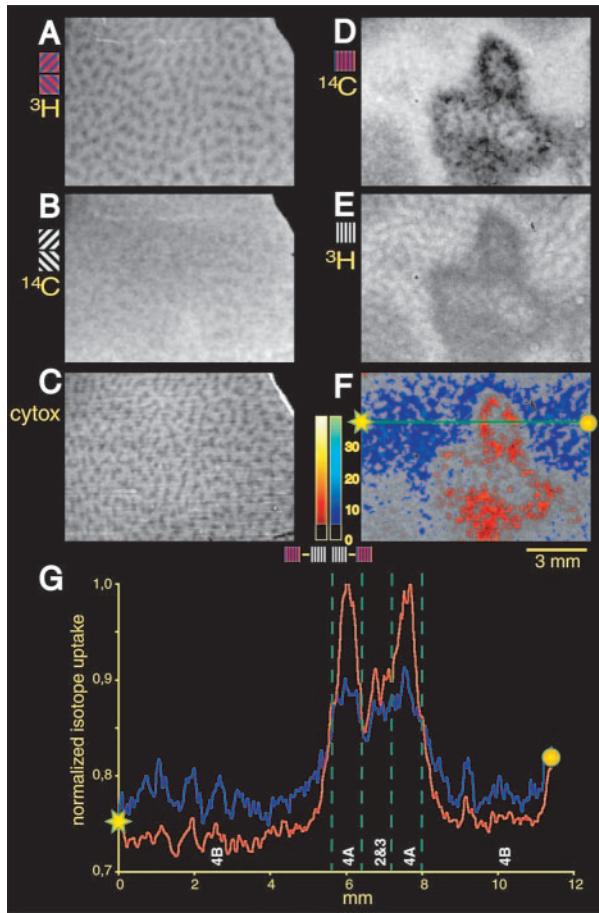
Figure 2. V1 topography of normalized 2L-DG uptake produced by equiluminant color-varying (*A* and *D*) and luminance-varying (*B* and *E*) stimuli, in different layers of V1. (*A*–*C*) are taken from a common section through layer 3, from case 3 (grating orientation varied). Color-varying uptake is much higher than luminance-varying uptake, and uptake is highest in the cytochrome oxidase blobs (*C*). (*D*) and (*E*) show analogous autoradiographs including lower layers, from a different case (no. 2, grating orientation constant). (*F*) A statistical map of *t* values (blue−cyan = luminance bias; red−yellow = color bias) differentiating (*D*) and (*E*) (*P* < 0.05, corrected for multiple comparisons; see pseudocolor scale bars). (*G*) A plot of normalized uptake along the blue line between the star and circle in (*F*). Color-driven uptake is relatively higher in layers 3 and 4A, whereas luminance-driven is much higher in layer 4B. Levels of DG uptake in stimulated layer 4B here were near-equivalent to those outside the visually stimulated region (not shown).

(Hubel *et al.*, 1978; Tootell and Hamilton, 1989; Ts'o *et al.*, 1990; Roe and Ts'o, 1995; Vanduffel *et al.*, 2002a,b), the gratings including a single local orientation (cases 1 and 2) produced orientation columns in the thick dark CO stripes, extending into the adjacent pale interstripes (see Fig. 3). Thus in V2, the regions of orientation selectivity correlated inversely with regions of high color sensitivity, as in macaque V1.

Areas VP and V4v

Beyond V2 in the macaque, there is little previous imaging data on color sensitivity. Figure 4 shows representative maps of color selectivity in VP (also known as V3v) and V4v. In both areas, we found discrete color-biased columns. These VP/V4v columns were rather wide and sparsely spaced (as in V2), but they were arranged in a less regular topography (compared with the systematic array in V2). In VP, the color-biased
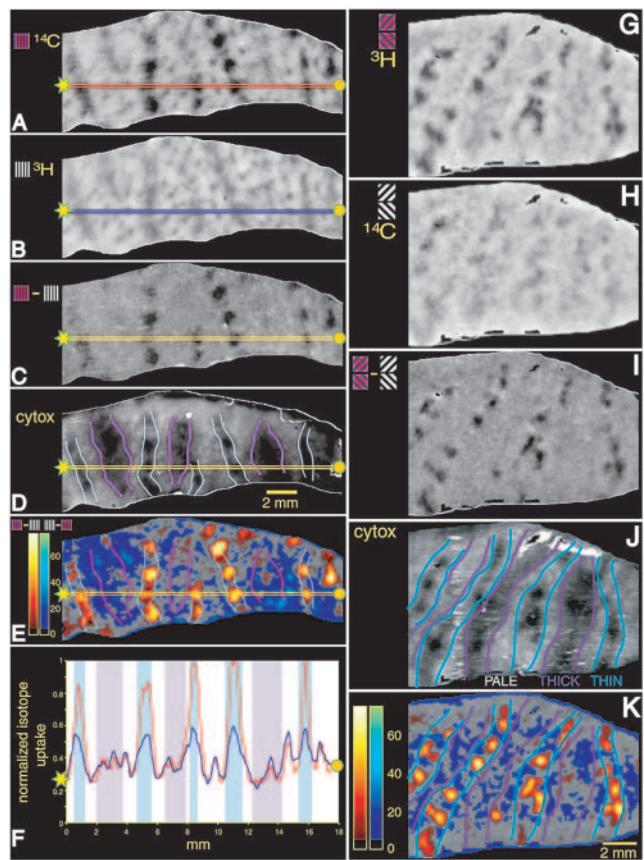

Figure 3. Topography of color-varying and luminance-varying uptake, and cytochrome oxidase stain, in V2, for case 2 (constant orientation, *A*–*F*) and case 3 (varied orientation, *G*–*K*). (*A*–*E*) and (*G*–*K*) were taken from sections cut parallel with the flattened surface of the postero-lateral lunate gyrus (fundus = lowermost; lip = uppermost). (*A*) and (*B*) (and *G* and *H*) are normalized autoradiographs produced by the equiluminant color-varying and luminance-varying gratings, respectively. (*C*) and (*I*) are the digital subtraction of (*B*) from (*A*), and (*H*) from (*G*), respectively (color bias = dark, luminance bias = light). (*D*) and (*J*) show the CO stain from the same tissue (thin and thick dark V2 'stripes' = blue and purple lines, respectively). (*E*) and (*K*) are statistical maps of *t* values (color-varying = red > yellow, luminance-varying = blue > cyan); CO stripes as in (*D*) and (*J*). Both pseudocolor scale bars are coded equivalently (*t* threshold > 4.6; *P* < 0.05). (*F*) shows a plot of normalized uptake (red = color-driven, blue = luminance-driven) measured between the star and dot in (*A*–*D*). The light blue and purple columns in (*F*) indicate the territory of thin and thick CO stripes, respectively. In case 2, the gratings were presented at a single (vertical) orientation. Thus the autoradiographs (*A* and *B*) reveal both the color-luminance differences, and the V2 orientation columns. The color-biased regions appear as dark stripes in (*C*), yellow−red regions in (*E*), and precipitous peaks in the 'red' line in (*F*) — all corresponding with the dark 'thin' CO stripes. Consistent with previous reports (Hubel and Livingstone, 1987; Tootell and Hamilton, 1989; DeYoe *et al.*, 1994; Vanduffel *et al.*, 2000), the orientation columns appeared as a regular matrix within the 'thick' and 'pale' CO stripes. Here, these orientation columns were activated near-equally by the color- and luminance-varying stimuli. Thus the red and blue lines were nearly coincident in the purple and white territory of (*F*), and these orientation columns were nearly eliminated by the digital subtraction in (*C*) and (*E*). However more detailed analysis showed that such columns and CO territories were activated slightly better by the luminance-varying stimuli. This marginal luminance bias appeared in the 'thick-' and 'pale' stripe territories, as a subtle white mottling in (*C*), a near-threshold 'blue' pseudocolor in (*E*), and a slight upward shift of the blue line in (*F*).

columns tended to be higher in contrast, and more numerous, compared with those in V4v.

Intriguingly, we also found isolated patches of higher (darker) CO activity in VP, V4v and V4d (see Figs 4 and 5). These isolated CO patches often showed higher color selec-
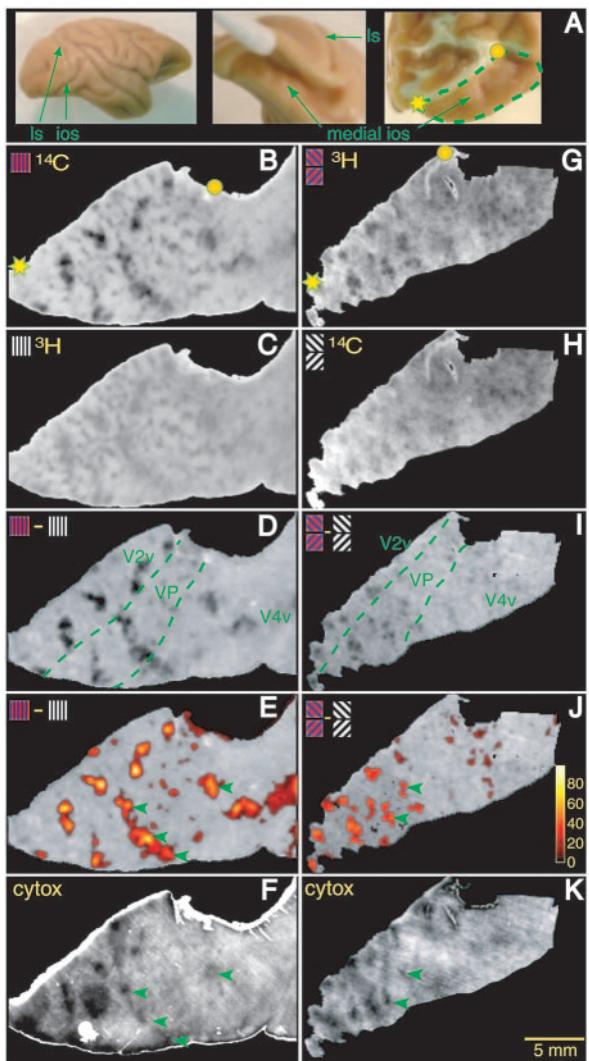
Figure 4. Topography of color-biased regions in VP and V4v, from the flattened ventromedial bank of the inferior occipital sulcus. (*A*) illustrates the approximate anatomical location of the tissue shown in (*B–F*) (ls = lunate sulcus; ios = inferior occipital sulcus), from a macaque used in a different study. The operculum (V1 + V2) was removed in the rightmost image. (*B*) and (*C*) show autoradiographs from the color-varying and luminance-varying conditions (respectively), from (orientation-specific) experiment 2. (*D*) is the subtraction image of (*B*) minus (*C*). Visual area borders (V2, VP, V4v) are indicated in dashed green lines. (*E*) is a statistical map of *t* values for color-biased regions (yellow > red); the luminance bias is not color-coded here. (*F*) shows the cytochrome oxidase stain from the same tissue. Some of the dark patches of CO staining in VP and V4v are color-biased (green arrows, *E* and *F*). (*G–K*) are from a different experiment (no. 3) in which the stimulus was presented at systematically varied ('all') orientations. Except for the corresponding lack of orientation columns in the raw autoradiographs (cf. *B* and *C*, *G* and *H*), the overall color-luminance differences are equivalent in the two cases.

tivity, when compared with the DG results from the same tissue (green arrows, Figs 4 and 5) — just as in the V2 thin stripes (Fig. 3). However, other CO and color-biased columns were *not* coincident, beyond V2.

Areas V3, V3A and V4d

Single units in macaque V3 (a.k.a. V3d) are reportedly direction-selective, with little overt color selectivity (Burkhalter *et al.*, 1986; Felleman and Van Essen, 1987; but see Gegenfurtner *et al.*, 1997). In fact, this relatively diminished color sensitivity was one of the defining functional properties distinguishing V3
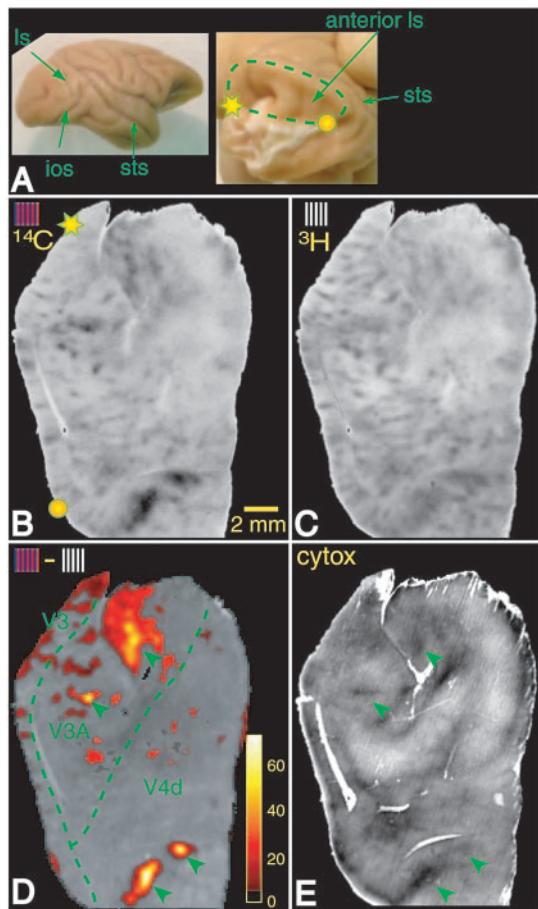

Figure 5. Topography of color-biased regions in dorsal V4, and adjacent areas V3 and V3a. (*A*) shows the location of the tissue in subsequent panels. (*B*) and (*C*) show the activity due to color- and luminance-varying stimuli (respectively), in experiments 2. (*D*) shows the color-biased regions after digital subtraction, as a *t*-value map. (*E*) shows the cytochrome oxidase stain of the same tissue. Green arrowheads in (*D*) and (*E*) show coincident regions of high CO and color bias. Color bias is largely absent from this large expanse of V4d, except for a distinctive column or two (bottom).

from area VP (V3v) (Burkhalter *et al.*, 1986). Consistent with this, we found comparatively little color bias in V3 (e.g. Figs 5 and 6), and V3 appeared less color-biased than VP (cf. Figs 4, 5 and 6). Relatively higher color bias was found in adjoining areas V3A anteriorly (e.g. Figs 5 and 6) and V2 posterio-laterally (Figs 3 and 4).

In V4d, where there have been so many conflicting reports about color selectivity, we found little overall color bias — even at the most forgiving statistical thresholds, across all six hemispheres tested. However a few large color-biased columns were found in V4d (e.g. yellow regions in Figs 5 and 6, and dark regions in Fig. 10). Interestingly, these few columns were located approximately where high percentages of color cells were reported many years ago by Zeki (1977) — in the anterior bank of the lunate sulcus (e.g. Figs 5 and 6), and the posterior bank of the superior temporal sulcus (Fig. 10). However because such color columns were so rare in V4, a larger sample would be necessary to confirm this observation.

TEO and TE

A recent hypothesis (see above) predicts that color-selective regions are located *anterior* to area V4, in/near macaque TEO,
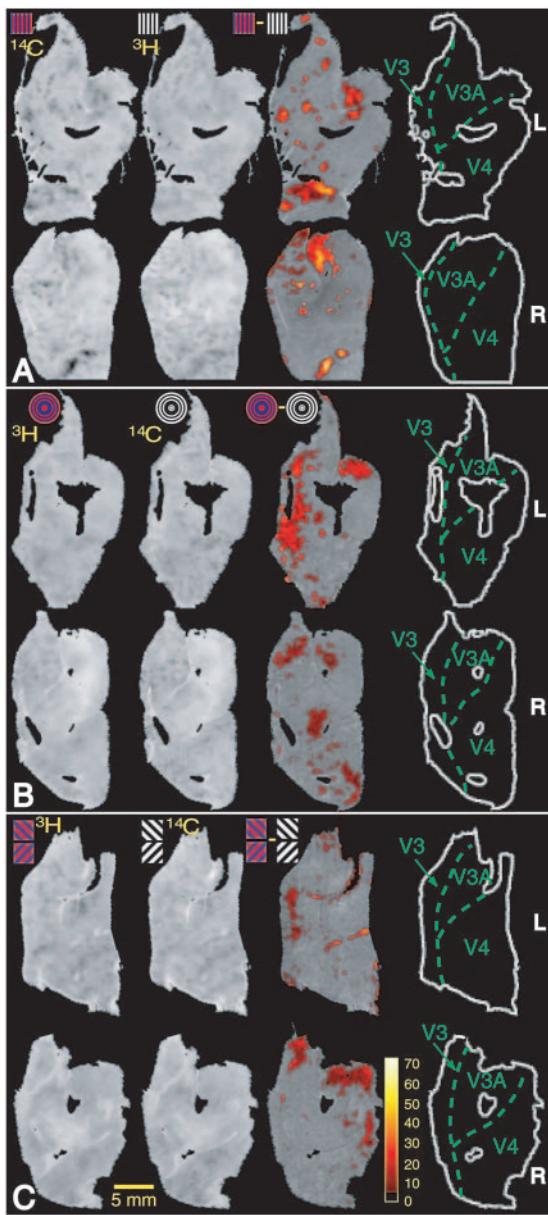
Figure 6. Color selectivity was not especially high in V4d, in any of the six hemispheres tested. Each panel shows the data from a given monkey, with left hemisphere shown above the right ('R' and 'L', respectively). Data from the left hemisphere has been mirror-reversed for ease of comparison. From left-to-right are shown the raw autoradiographs for color-varying then luminance-varying gratings, then the statistical map of *t* values for the color biased regions (see pseudocolor scale), then a diagram of the estimated cortical area boundaries for each of the individual samples. As elsewhere, the pseudocolor scale is thresholded at $P < 0.05$, corrected. A few isolated color-biased columns (yellow in *A*), and a few additional regions of marginal color selectivity (red in *B* and *C*) were seen in V4d, but most of V4d did not show color bias. Overall, comparatively higher color bias was present in V3A.

and perhaps further anterior in TE. Remarkably, we did find higher color selectivity, in both these predicted regions (Figs 7–9). Although there was some variability in the size and amplitude of these color-biased patches, the color selectivity was statistically significant in both regions, in all six hemispheres tested. One patch of color-biased activity (~TEO) lay between the posterior middle temporal sulcus (PMTS) and the anterior fundus of the inferior occipital sulcus. A more anterior patch of
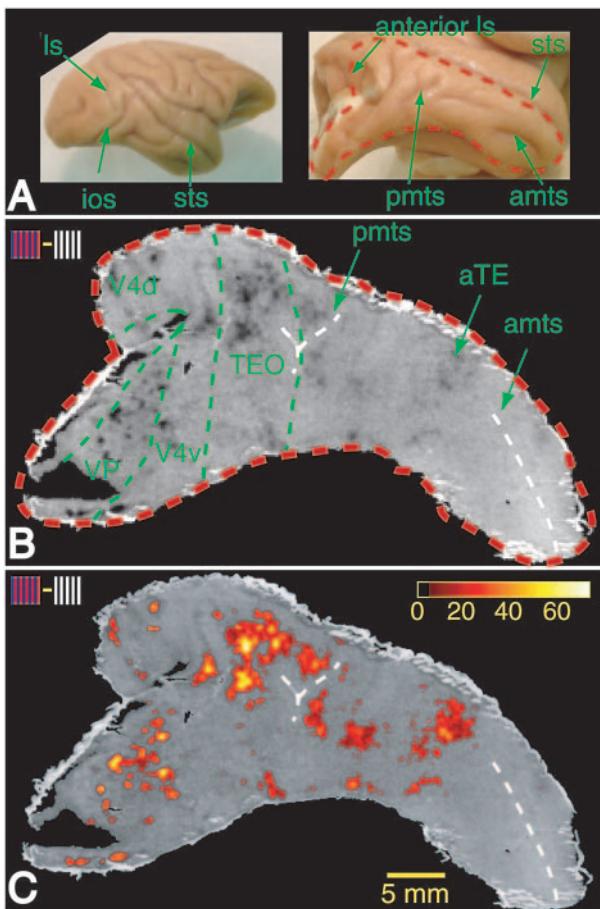

Figure 7. Topography of color selectivity on the inferior temporal gyrus, and neighboring regions. (*A*) shows the anatomical region illustrated below. (*B*) shows the digital subtraction between activity produced by color- and luminance-varying gratings (dark = color bias; light = luminance bias), with area and sulcal boundaries labeled. (*C*) shows the *t* values for the color bias in the same section.
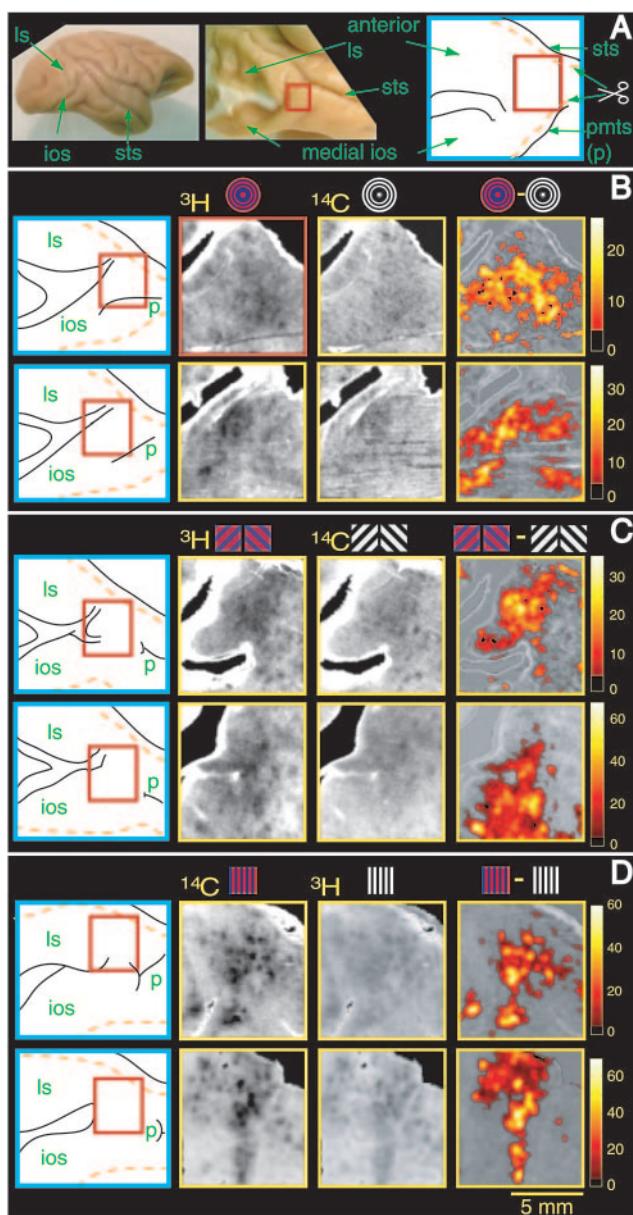
color-biased activity lay just posterior to the posterior terminus of the anterior middle temporal sulcus (AMTS); for convenience we will refer to it as 'aTE' (without assuming it is a genuine cortical area).

Near threshold (at 'red' pseudocolor values), the patches of significant color selectivity in ~TEO and aTE often merged together (see Figs 7–9). However, closer inspection of the raw autoradiographs, and the regions of highest color bias (yellow pseudocolor) in the same figures, showed that the *most robust* color-selective activity was segregated into multiple distinct columns.

Areas MT and STS

Previous single unit reports (e.g. Thiele *et al.*, 2001) and the results in layer 4B of V1 (e.g. Fig. 2) predict a significant *luminance* bias in the MT response, at least in response to moving stimuli. This hypothesis was confirmed in case 1, in which the stimuli were moving (see Fig. 10).
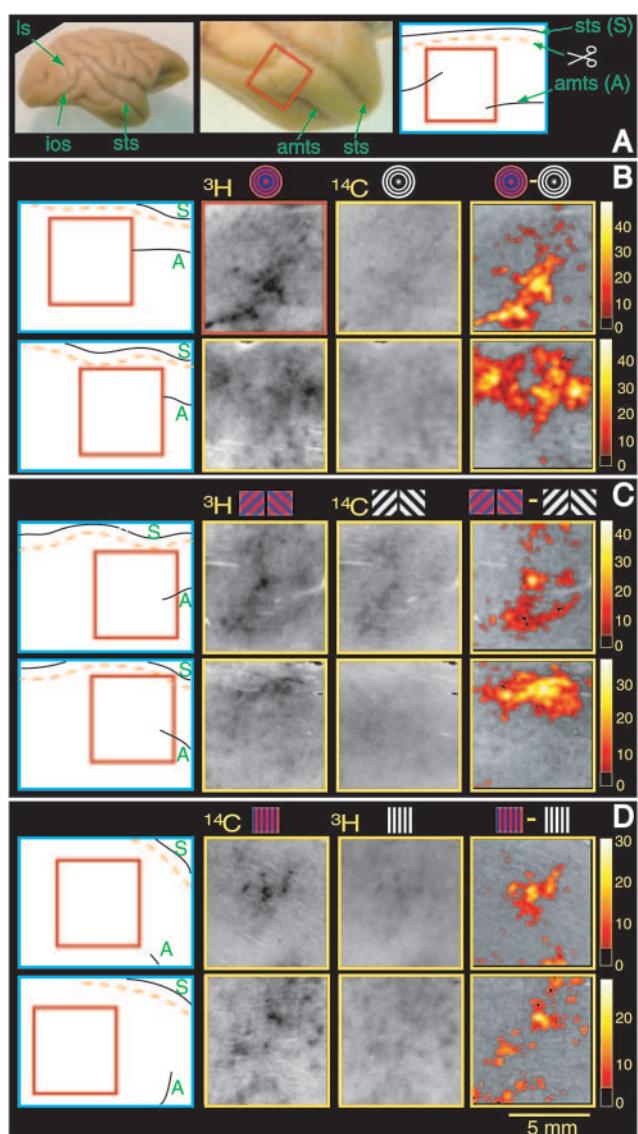
In the other two cases we used stationary stimuli, which produced low uptake to both color and luminance stimuli. Both the luminance bias, and the greater response to moving stimuli, were entirely consistent with previous studies of MT in macaque, and MT(+) in humans. In this study, we saw few luminance biases elsewhere in extrastriate cortex.

Figure 8. Color selectivity in/near TEO, in all six hemispheres tested. (*A*) illustrates the rectangular region sampled, between PMTS and the fundus of the anterior inferior occipital sulcus. (*B*), (*C*) and (*D*) show data from experiments 1–3 (respectively), from right and left hemispheres of each experiment. In each row, from left to right are illustrated: (1) the individual gyral/sulcal anatomy of each sampled region; (2), (3) the autoradiographs from the color- and luminance-varying conditions, respectively, and (4) the *t* value maps of the color-biased regions, after digital subtraction.

Figure 9. Color selectivity in anterior superior temporal sulcus. The format is similar to that in Figure 8, except that the sampled region was located just posterior to the anterior middle temporal sulcus, in TE cortex.

Discussion

A Color 'Center' in Primate Visual Cortex?

In primate visual cortex, it has been attractive to think in terms of a specific color center (one main area, plus perhaps related areas), in the way that area MT (and its satellites) are considered a primary center for visual motion processing. However prior evidence for such a color center has been difficult to evaluate, because it has been based on different techniques, from different visual cortical areas, in different (human and non-human) species.

In some ways, the human data are the most straightforward to interpret. Clinical damage to a cortical region in/near the fusiform/lingual gyri in occipitotemporal cortex causes an intriguing deficit called 'achromatopsia' in which the visual world appears permanently colorless, like 'various shades of gray', or 'dirty snow' (Pearlman *et al.*, 1979; Damasio *et al.*, 1980). This intriguing perceptual deficit was attributed to damage in a color-processing 'center' in that brain location.

Subsequent neuroimaging studies in normal subjects confirmed the presence of color-related activity in the same cortical location, named variously 'V4' (Lueck *et al.*, 1989; Zeki, 1990; McKeefry and Zeki, 1997; Bartels and Zeki, 2000), 'V8' (Hadjikhani *et al.*, 1998; Tootell and Hadjikhanim, 2001) or 'VO' (Wandell, 1999). There is no disagreement about the presence and location of this small color-selective area 'V4' (Lueck *et al.*, 1989; McKeefry and Zeki, 1997; Hadjikhani *et al.*, 1998; Beauchamp *et al.*, 1999; Bartels and Zeki, 2000) or
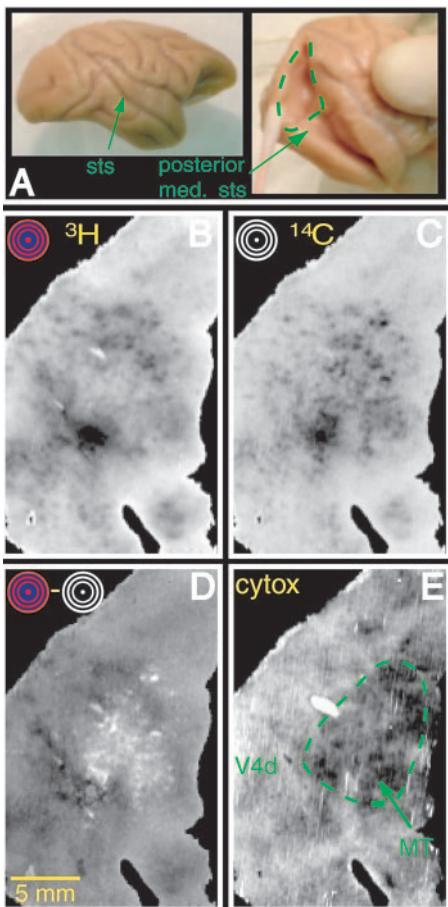
Figure 10. Topography of color- and luminance-driven activity in MT and surrounding cortex. The tissue is sampled from the posterior bank and fundus of the dorsal superior temporal sulcus (see A). (*B*) and (*C*) show autoradiographs produced by the moving color- and luminance-varying grating (no. 1), respectively. (*D*) is the achromatic difference image (dark = color bias; white = luminance bias). (*E*) is the cytochrome oxidase stain, including the CO patches distinguishing MT. A distinctive region of high luminance bias is found within MT. A few isolated color-biased columns can be seen in V4d.

related anterior regions (Beauchamp *et al.*, 1999; Bartels and Zeki, 2000). However the retinotopy in and around this region (which helps define the macaque–human homology) is currently under spirited discussion.

Direct comparisons of the human and macaque maps (Hadjikhani *et al.*, 1998; Van Essen *et al.*, 2001) predicts that any hypothetical (color-selective) homologues of the human color area (and satellites) should be located in/near *macaque* TEO and anterior TE, respectively. This prediction was confirmed here (Figs 7–9). One color-selective patch was in/near TEO, as mapped electrophysiologically (Boussaoud *et al.*, 1991) – just posterior to the PMTS, and anterior to V4 (Figs 7 and 8). The second patch was located ~2 cm further anterior on the inferior temporal gyrus (Fig. 9).

Previous results support the color selectivity we found in these regions. For instance, experimental lesions in macaque TE/TEO can produce behavioral evidence for a macaque 'achromatopsia' (Heywood *et al.*, 1995; Huxlin *et al.*, 2000). Furthermore, discrete patches of color-selective cells were reported in/near 'aTE', well before we found such regions here (Komatsu *et al.*, 1992). Our findings here are also consistent with a PET study of attention to color in monkeys (Takechi *et*

al., 1997), although color sensitivity *per se* was not tested in that study.

Early single unit studies from one investigator (Zeki, 1973, 1977) reported that macaque V4(d) is color-selective. However subsequent quantitative studies concluded that macaque V4d units are *not* especially color-selective (Kruger and Gouras, 1980; Fischer *et al.*, 1981; Van Essen *et al.*, 1981; Schein *et al.*, 1982). A recent study agreed in general, but allowed for the possibility of 'hidden' color selectivity in V4 (Schein and Desimone, 1990). However, subsequent studies found similar 'hidden' color selectivity in V1 (Wachtler *et al.*, 2001) – which only re-emphasized the lack of unique color specificity in V4d.

Moreover, lesions of V4d did *not* produce fundamental deficits in color perception (Heywood and Cowey, 1987; Heywood *et al.*, 1992; Schiller, 1993; Walsh *et al.*, 1993). Thus we were not surprised to find only low-to-moderate color-bias in the present 2L-DG results from V4d (Figs 4–7).

Color Architecture in Lower-tier Areas

The present results strongly support the 'classical' blob-and-thin-stripe model of color-processing architecture in V1 and V2 (Livingstone and Hubel, 1984; Hubel and Livingstone, 1987; Ts'o and Gilbert, 1988; Tootell and Hamilton, 1989; DeYoe *et al.*, 1994; Roe and Ts'o, 1999; Landisman and Ts'o, 2002; Moutoussis and Zeki, 2002). However, some single unit reports have not completely confirmed this classical organization (Lennie *et al.*, 1990; Peterhans and von der Heydt, 1993; Levitt *et al.*, 1994; Leventhal *et al.*, 1995; Yoshioka and Dow, 1996; Kiper *et al.*, 1997). How can these discrepant single unit reports be reconciled with the profound and unambiguous organization revealed in the functional anatomy (e.g. Figs 2 and 3)?

One obvious consideration is that single unit sampling is statistically more noisy, compared with functional maps which reflect the activity of thousands or millions of neurons at one time. For instance, one electrophysiological study of color in macaque V1 described only eight histologically confirmed single units within CO blobs (Lennie *et al.*, 1990). Another possibility is that the dendrites (which contribute more to the DG and optical signals) have a more orderly functional organization, compared with the neuronal somas (recorded by the extracellular microelectrodes) which are embedded within this matrix.

Architecture of Color Columns Beyond V1/V2

Where it was present, the limited color-selective activity in V4 was segregated into discrete, relatively large columns, in both V4d (Figs 5, 6 and 10) and V4v (Fig. 4). Other studies (Zeki, 1973; DeYoe *et al.*, 1994; Xiao *et al.*, 1999) also support our current DG evidence for large and isolated color-selective columns in V4. With hindsight, one can imagine how a misleading impression of high color selectivity could have arisen from a series of fortuitous (or unfortunate) single unit probes into such large column(s) in V4d.

In area(s) VP, V4v and V4d, the color columns were often coincident with dark patches of cytochrome oxidase staining (e.g. Figs 4 and 5). This is strikingly reminiscent of analogous relationships in the V1 blobs and the V2 thin stripes (e.g. Figs 2, 3 and 10). However, in V1 and V2 the CO-color patches are essentially always coincident, whereas only some of the CO and color patches were aligned in V4d, V4v and VP. In V4, those coincident regions may receive specific cortical connec-

tions from the V2 thin stripes (DeYoe *et al.*, 1994; Xiao *et al.*, 1999).

We had no preconceptions about possible columnar architectures underlying color or luminance sensitivity, but several generalities emerged from the data. Typically, the color-biased activity took the form of discrete patches or isolated columns. Outside these color-biased regions, cortex had a more balanced sensitivity to luminance and color, slightly biased towards luminance in our stimulus configuration. These 'non-color-bias' regions were topographically diffuse and widespread, rather than segregated in discrete, isolated columns (e.g. Fig. 3). We found few examples of alternative possibilities (e.g. strongly luminance-biased columns, or topographically diffuse color biases). Simplistically, the general pattern was of isolated color-selective 'islands' in a sea of cortex that was responsive to both luminance and color. Magnocellular-influenced area MT (Fig. 10) and layer 4B of V1 (Fig. 2) were the notable exceptions to this rule.

The topography of the color columns showed an interesting trend, when revealed like this across different levels of the visual cortical hierarchy. Recall that in V1, the color-biased 'blobs' form a regular, tightly packed, two-compartment (blob/interblob) array (Fig. 2). In V2, the color-biased columns (basically, the thin stripes) become relatively larger and more widely spaced, in a more complex three-compartment (thin/thick/interstripe) matrix (e.g. Fig. 3). In higher-tier areas (especially VP, V3A and V4d/v), we found that this general tendency continued: the DG-labeled color columns were typically spaced sparsely and/or irregularly relative to each other (Figs 4–7 and 10), and the color columns were sometimes quite large. Anterior to V4, some of the columns were 're-grouped' into functional domains (patches of columns) (Figs 7–9) but the columnar topography never returned to a repeating, regularly spaced array (as in V1).

What would produce such topographic changes? One possibility is that more stimulus dimensions (or more complicated dimensions) are coded in correspondingly more columnar systems, in progressively higher-tier areas (e.g. Fujita *et al.*, 1992). Thus in higher-tier areas, the label for a given single type of column (e.g. color) will be 'crowded out' by the additional columnar systems, hence appearing more sparsely spaced, and/or irregularly arrayed. This model is consistent with the well-known transformation of simpler retinotopic information (e.g. V1, V2) into more complex information coding (e.g. IT cortex) along the same hierarchy.

This idea also rationalizes an otherwise-puzzling aspect of the color topography. Even in those areas which are demonstrably retinotopic (e.g. V1, V2, V3, V3A, etc.), regions of high color selectivity occupy only a subset of the cortical surface area (e.g. ~30% of the surface area in the V1 upper layers, ~23% of the surface area in V2, etc.). With normal trichomatic vision, there is a much wider range of discriminable variation in color than in luminance, at each point in the visual field: shouldn't this lead to relatively *more* color columns in these retinotopic areas? However, since the spatial resolution of the color system is so much lower than that of the luminance-based system (e.g. Van der Horst and Bouman, 1969; Granger and Heurtley, 1973; Watanabe *et al.*, 1976; Mullen, 1985), presumably many fewer neurons are required to 'cover' equivalent regions of the visual field for color, compared with the number of neurons required for the high-resolution luminance system. This difference in

spatial resolution would thus rationalize the relatively sparse distribution of color columns, even in retinotopic areas.

Stimulus Limitations
Our stimuli spanned luminance contrasts and color contrasts that were both as large as possible, given the physical constraints involved. Due to the different nature of color and luminance processing, this meant that our effective cone contrast was much (~1 log unit) larger for the luminance-varying stimulus, compared to that of the color-varying stimulus. Despite this luminance bias in the cone contrast, the columns we uncovered were almost all selective for color rather than luminance. Presumably this color bias would have been even greater if we had equated for cone contrast, rather than for luminance.

The grating stimuli used here probably did not optimally activate all cells in inferotemporal (IT) cortex. It is well accepted that IT single units often respond best to more complicated stimuli. However, most IT cells respond best to *different* complex stimuli. Thus it was not clear how to optimize our stimuli for all IT cells, nor how to avoid chromatic aberration in such complicated stimuli, etc. In IT cortex, it is gratifying that we were able to reveal as much color- and luminance-biased activity as we did (e.g. Figs 7–9).

Which 'Primate' Visual Cortex?
In this study, we found a reassuring correspondence in the cortical maps of color selectivity, in humans compared with macaques. Many previously confusing details were resolved here by testing two simple hypotheses: macaque color maps are (i) different than proposed previously, but (ii) equivalent to those in humans. In other comparisons between macaque and human cortical maps, correspondence has also been the rule rather than the exception. However, specific human–macaque differences are also becoming more well-documented (e.g. Vanduffel *et al.*, 2002b; Fize *et al.*, 2003; Tootell *et al.*, 2003).

Current assumptions about 'primate' vision are based on an uncalibrated mix of data from both humans and macaques. To specify exactly how primate visual cortex works, it will be crucial to sort out exactly how visual cortex differs in these two families, and which features remain constant, across ~30 million years of independent evolution.

References
Albright TD, Desimone R, Gross CG (1984) Columnar organization of directionally selective cells in visual area MT of the macaque. J Neurophysiol 51:16–31.

Bartels A, Zeki S (2000) The architecture of the colour centre in the human visual brain: new results and a review. Eur J Neurosci 12:172–193.

Beauchamp MS, Haxby JV, Jennings JE, DeYoe EA (1999) An fMRI version of the Farnsworth–Munsell 100-Hue test reveals multiple color-selective areas in human ventral occipitotemporal cortex. Cereb Cortex 9:257–263.

Boussaud D, Desimone R, Ungerleider LG (1991) Visual topography of area TEO in the macaque. J Comp Neurol 306:554–575.

Buckley MJ, Gaffan D, Murray EA (1997) Functional double dissociation between two inferior temporal cortical areas: perirhinal cortex versus middle temporal gyrus. J Neurophysiol 77:587–598.

Burkhalter A, Felleman DJ, Newsome WT, Van Essen DC (1986) Anatomical and physiological asymmetries related to visual areas V3 and VP in macaque extrastriate cortex. Vision Res 26:63–80.

Damasio A, Yamada T, Damasio H, Corbett J, McKee J (1980) Central achromatopsia: behavioral, anatomic, and physiologic aspects. Neurology 30:1064–1071.

De Valois RL, Snodderly DM, Yund EW, Hepler NK (1977) Responses of macaque lateral geniculate cells to luminance and color figures. Sens Processes 1:244–259.

DeYoe EA, Felleman DJ, Van Essen DC, McClendon E (1994) Multiple processing streams in occipitotemporal visual cortex. Nature 371:151–154.

Dobkins KR, Thiele A, Albright TD (2000) Comparison of red-green equiluminance points in humans and macaques: evidence for different L:M cone ratios between species. J Opt Soc Am A Opt Image Sci Vis 17:545–556.

Felleman DJ, Van Essen DC (1987) Receptive field properties of neurons in area V3 of macaque monkey extrastriate cortex. J Neurophysiol 57:889–920.

Fischer B, Boch R, Bach M (1981) Stimulus versus eye movements: comparison of neural activity in the striate and prelunate visual cortex (A17 and A19) of trained rhesus monkey. Exp Brain Res 43:69–77.

Fize D, Vanduffel W, Nelissen K, Denys K, Chef d'Hotel C, Faugeras O, Orban G (2003) The retinotopic organization of primate dorsal V4 and surrounding areas: a functional magnetic resonance imaging study in awake monkeys. J Neurosci 23:7395–7406.

Fujita I, Tanaka K, Ito M, Cheng K (1992) Columns for visual features of objects in monkey inferotemporal cortex. Nature 360:343–346.

Gattass R, Sousa AP, Gross CG (1988) Visuotopic organization and extent of V3 and V4 of the macaque. J Neurosci 8:1831–1845.

Geesaman BJ, Born RT, Andersen RA, Tootell RB (1997) Maps of complex motion selectivity in the superior temporal cortex of the alert macaque monkey: a double-label 2-deoxyglucose study. Cereb Cortex 7:749–757.

Gegenfurtner KR, Kiper DC, Levitt JB (1997) Functional properties of neurons in macaque area V3. J Neurophysiol 77:1906–1923.

Granger EM, Heurtley JC (1973) Visual chromaticity modulation-transfer function. J Opt Soc Am 63:1173–1174.

Hadjikhani N, Liu AK, Dale AM, Cavanagh P, Tootell RB (1998) Retinotopy and color sensitivity in human visual cortical area V8. Nat Neurosci 1:235–241.

Heywood CA, Cowey A (1987) On the role of cortical area V4 in the discrimination of hue and pattern in macaque monkeys. J Neurosci 7:2601–2617.

Heywood CA, Gadotti A, Cowey A (1992) Cortical area V4 and its role in the perception of color. J Neurosci 12:4056–4065.

Heywood CA, Gaffan D, Cowey A (1995) Cerebral achromatopsia in monkeys. Eur J Neurosci 7:1064–1073.

Hicks TP, Lee BB, Vidyasagar TR (1983) The responses of cells in macaque lateral geniculate nucleus to sinusoidal gratings. J Physiol (Lond) 337:183–200.

Hubel DH, Livingstone MS (1987) Segregation of form, color, and stereopsis in primate area 18. J Neurosci 7:3378–3415.

Hubel DH, Wiesel TN, Stryker MP (1978) Anatomical demonstration of orientation columns in macaque monkey. J Comp Neurol 177:361–380.

Huxlin KR, Saunders RC, Marchionini D, Pham HA, Merigan WH (2000) Perceptual deficits after lesions of inferotemporal cortex in macaques. Cereb Cortex 10:671–683.

Kiper DC, Fenstemaker SB, Gegenfurtner KR (1997) Chromatic properties of neurons in macaque area V2. Vis Neurosci 14:1061–1072.

Komatsu H, Ideura Y, Kaji S, Yamane S (1992) Color selectivity of neurons in the inferior temporal cortex of the awake macaque monkey. J Neurosci 12:408–424.

Kruger J, Gouras P (1980) Spectral selectivity of cells and its dependence on slit length in monkey visual cortex. J Neurophysiol 43:1055–1069.

Landisman CE, Ts'o DY (2002) Color processing in macaque striate cortex: relationships to ocular dominance, cytochrome oxidase, and orientation. J Neurophysiol 87:3126–3137.

Lennie P, Krauskopf J, Sclar G (1990) Chromatic mechanisms in striate cortex of macaque. J Neurosci 10:649–669.

Leventhal AG, Thompson KG, Liu D, Zhou Y, Ault SJ (1995) Concomitant sensitivity to orientation, direction, and color of cells in layers 2, 3, and 4 of monkey striate cortex. J Neurosci 15:1808–1818.

Levitt JB, Kiper DC, Movshon JA (1994) Receptive fields and functional architecture of macaque V2. J Neurophysiol 71:2517–2542.

Livingstone MS, Hubel DH (1984) Anatomy and physiology of a color system in the primate visual cortex. J Neurosci 4:309–356.

Lueck CJ, Zeki S, Friston KJ, Deiber MP, Cope P, Cunningham VJ, Lammertsma AA, Kennard C, Frackowiak RS (1989) The colour centre in the cerebral cortex of man. Nature 340:386–389.

Malonek D, Tootell RB, Grinvald A (1994) Optical imaging reveals the functional architecture of neurons processing shape and motion in owl monkey area MT., Proc R Soc Lond B Biol Sci 258:109–119.

McKeefry DJ, Zeki S (1997) The position and topography of the human colour centre as revealed by functional magnetic resonance imaging. Brain 120:2229–2242.

Moutoussis K, Zeki S (2002) Responses of spectrally selective cells in macaque area V2 to wavelengths and colors. J Neurophysiol 87:2104–2112.

Mullen KT (1985) The contrast sensitivity of human colour vision to red-green and blue-yellow chromatic gratings. J Physiol (Lond) 359:381–400.

Pearlman AL, Birch J, Meadows JC (1979) Cerebral color blindness: an acquired defect in hue discrimination. Ann Neurol 5:253–261.

Peterhans E, von der Heydt R (1993) Functional organization of area V2 in the alert macaque. Eur J Neurosci 5:509–524.

Previc FH (1986) Visual evoked potentials to luminance and chromatic contrast in rhesus monkeys. Vision Res 26:1897–1907.

Roe AW, Ts'o DY (1995) Visual topography in primate V2: multiple representation across functional stripes. J Neurosci 15:3689–3715.

Roe AW, Ts'o DY (1999) Specificity of color connectivity between primate V1 and V2. J Neurophysiol 82:2719–2730.

Schein SJ, Marrocco RT, de Monasterio FM (1982) Is there a high concentration of color-selective cells in area V4 of monkey visual cortex? J Neurophysiol 47:193–213.

Schein SJ, Desimone R (1990) Spectral properties of V4 neurons in the macaque. J Neurosci 10:3369–3389.

Schiller PH (1993) The effects of V4 and middle temporal (MT) area lesions on visual performance in the rhesus monkey. Vis Neurosci 10:717–746.

Takechi H, Onoe H, Shizuno H, Yoshikawa E, Sadato N, Tsukada H, Watanabe Y (1997) Mapping of cortical areas involved in color vision in non-human primates. Neurosci Lett 230:17–20.

Thiele A, Dobkins KR, Albright TD (2001) Neural correlates of chromatic motion perception. Neuron 32:351–358.

Thorell LG, De Valois RL, Albrecht DG (1984) Spatial mapping of monkey V1 cells with pure color and luminance stimuli. Vision Res 24:751–769.

Tootell RB, Silverman MS, Hamilton SL, De Valois RL, Switkes E (1988) Functional anatomy of macaque striate cortex. III. Color. J Neurosci 8:1569–1593.

Tootell RB, Hamilton SL (1989) Functional anatomy of the second visual area (V2) in the macaque. J Neurosci 9:2620–2644.

Tootell RB, Hadjikhanim N (2001) Where is 'dorsal V4' in human visual cortex? Retinotopic, topographic and functional evidence. Cereb Cortex 11:298–311.

Tootell RB, Tsao D, Vanduffel W (2003) Neuroimaging weighs in: humans meet macaques in 'primate' visual cortex. J Neurosci 23:3981–3989.

Ts'o DY, Gilbert CD (1988) The organization of chromatic and spatial interactions in the primate striate cortex. J Neurosci 8:1712–1727.

Ts'o DY, Frostig RD, Lieke EE, Grinvald A (1990) Functional organization of primate visual cortex revealed by high resolution optical imaging. Science 249:417–420.

Van der Horst GJC, Bouman MA (1969) Spatio-temporal chromaticity discrimination. J Opt Soc Am 59: 1482–1488.

Vanduffel W, Tootell RB, Orban GA (2000) Attention-dependent suppression of metabolic activity in the early stages of the macaque visual system. Cereb Cortex 10:109–126.

Vanduffel W, Tootell RB, Schoups AA, Orban GA (2002a) The organization of orientation selectivity throughout macaque visual cortex. Cereb Cortex 12:647–662.

Vanduffel W, Fize D, Peuskens H, Denys K, Sunaert S, Todd JT, Orban GA (2002b) Extracting 3D from motion: differences in human and monkey intraparietal cortex. Science 298:413–415.

Van Essen DC, Zeki SM (1978) The topographic organization of rhesus monkey prestriate cortex. J Physiol (Lond) 277:193–226.

Van Essen DC, Maunsell JH, Bixby JL (1981) The middle temporal visual area in the macaque: myeloarchitecture, connections, functional properties and topographic organization. J Comp Neurol 199:293–326.

Van Essen DC, Lewis JW, Drury HA, Hadjikhani N, Tootell RB, Bakircioglu M, Miller MI (2001) Mapping visual cortex in monkeys and humans using surface-based atlases. Vision Res 41:1359–1378.

Wachtler T, Albright TD, SejnowskiTJ (2001) Nonlocal interactions in color perception: nonlinear processing of chromatic signals from remote inducers. Vision Res 41:1535–1546.

Walsh V, Carden D, Butler SR, Kulikowski JJ (1993) The effects of V4 lesions on the visual abilities of macaques: hue discrimination and colour constancy. Behav Brain Res 53:51–62.

Wandell BA (1999) Computational neuroimaging of human visual cortex. Annu Rev Neurosci 22:145–173.

Watanabe A, Sakata H, Isono H (1976) Chromatc spatial sine wave response of the human visual system. NHK Lab Note 198:1–10.

Worsley KJ, Marrett S, Neelin P, Vandal AC, Friston KJ, Evans AC (1996) A unified statistical approach for determining significant signals in images of cerebral activation. Hum Brain Mapp 4:58–73.

Xiao Y, Zych A, Felleman DJ (1999) Segregation and convergence of functionally defined V2 thin stripe and interstripe compartment projections to area V4 of macaques. Cereb Cortex 9:792–804.

Xiao Y, Wang Y, Felleman DJ (2003) A spatially organized representation of colour in macaque cortical area V2. Nature 421:535–539.

Yoshioka T, Dow BM (1996) Color, orientation and cytochrome oxidase reactivity in areas V1, V2 and V4 of macaque monkey visual cortex. Behav Brain Res 76:71–88.

Zeki SM (1973) Colour coding in rhesus monkey prestriate cortex. Brain Res 53:422–427.

Zeki SM (1977) Colour coding in the superior temporal sulcus of rhesus monkey visual cortex. Proc R Soc Lond B Biol Sci 197:195–223.

Zeki S (1990) A century of cerebral achromatopsia. Brain 113:1721–1777.